34th Annual International Conference of the IEEE EMBS
San Diego, California USA, 28 August - 1 September, 2012

3D Cardiac Motion Reconstruction from CT Data and Tagged MRI

Xiaoxu Wang[1], Viorel, Mihalef[2], Zhen Qian, Szilard Voros [3], Dimitris Metaxas[4]

Abstract— **In this paper we present a novel method for left ventricle (LV) endocardium motion reconstruction using high resolution CT data and tagged MRI. High resolution CT data provide anatomic details on the LV endocardial surface, such as the papillary muscle and trabeculae carneae. Tagged MRI provides better time resolution. The combination of these two imaging techniques can give us better understanding on left ventricle motion. The high resolution CT images are segmented with mean shift method and generate the LV endocardium mesh. The meshless deformable model built with high resolution endocardium surface from CT data fit to the tagged MRI of the same phase. 3D deformation of the myocardium is computed with the Lagrangian dynamics and local Laplacian deformation. The segmented inner surface of left ventricle is compared with the heart inner surface picture and show high agreement. The papillary muscles are attached to the inner surface with roots. The free wall of the left ventricle inner surface is covered with trabeculae carneae. The deformation of the heart wall and the papillary muscle in the first half of the cardiac cycle is presented. The motion reconstruction results are very close to the live heart video.**

I. Introduction

Early diagnosis of cardiovascular diseases with the aid of medical imaging technology and early treatment of these diseases can greatly reduce the risk of diseases. Medical image technology such as Computed Tomography (CT) and tagged Magnetic Resonance Image (tagged MRI) provide a non-invasive way to view anatomic structure and motion of the atria and ventricles. The multi-detector CT with high rotation speed provides a high resolution view of heart wall, especially the detailed anatomic structures such as papillary muscle and trabeculae carneae on ventricle endocardial surface. The papillary muscles are attached to the mitral valves with some tissue and help to keep the mitral valve from being inverted when the blood pressure rises inside the ventricles. The dysfunction of the papillary muscles due to ischemia or infarction can adversely affect cardiac function through the insufficient strain on mitral valves. The deformation of the papillary muscles causes great interest in cardiovascular disease research (Axel 2004) [1]. The time resolution of CT is about one third of TMRI. The CT data we have has 10 frames in a heart beating cycle, while tagged MRI data has 30 frames. Besides better time resolution, with tagging techniques, taggedMRI can show not only the surface deformation, but also the in-wall myocardium motion such as the twisting in the short Axis circumferential direction. With meshless deformable models, the motion of myocardium can be reconstructed from tagged MRI. The deformation of detailed anatomic structure such as papillary muscle and trabeculae carneae cannot be achieved solely based on MRI. The LV endocardium directly contracts the blood and pump to the whole body. Their deformation can provide information for blood flow simulation in the LV.

A lot of research has been dedicated to heart reconstruction from CT data. Chen et al. 2004 [2] reconstructed the whole heart from high resolution CT data, with the emphasis on the ventricle endocardial surfaces. His experimental results further proved that the papillary muscles are attached on the trabeculae carneae lining the ventricle wall instead of directly on the solid wall (Axel 2004 [1]). Ionasec et al. 2008 [3] built a 4D physiological model, which combines learning-based technologies into a coarse-to-fine approach, to reconstruct the aorta valve (AV) motion based on the CT data. Zheng et al. 2008 [4] built a four-chamber heart model from the automatic segmentation results of cardiac CT volumes. In their work, 3D CT volumes are segmented with marginal space learning and a mesh fits onto the data with corresponding landmarks. Their mesh does not keep the detailed structure on endocardial surfaces.

Deformable models (Metaxas et al. 1991 [5]) have been used for motion reconstruction from tagged MRI for a long time. J. Park et al. 1995 [6] presented deformable models to track the LV motion. K. Park et al. 2003 [7] further extended cardiac deformable models to recover the right ventricle (RV) motion and conduct 4D cardiac functional analysis using Finite Element Methods (FEM). Recently meshless deformable models [8, 9] were developed for LV motion reconstruction. The 3D motion field is computed and updated using the Lagrange equation. The external force is extracted from tagged MRI. The left ventricle model is deformed with meshless deformable models.

3D Strain field is computed with moving least squares. We propose a novel dynamic deformable model for LV endocardium motion reconstruction. A CT frame at the end of diastole is chosen as the reference frame since the heart is the most static at this moment. Meanshift method with both the intensity and spatial information was used to segment the 3D volume. We fit the inner surface reconstructed from CT data, with a meshless deformable model, onto the tagged MRI data. The meshless deformable model deforms using the Lagrange equation as in [8, 9].

Our paper is organized as follows. Section 2 introduces the new model: 3D volume segmentation, mesh generation, and

Xiaoxu Wang[1] are with the Shenzhen Institute of Advanced Technology, Chinese Academy of Sciences, Hongkong Chinese University, Ave. 1068, Xili, Shenzhen, Guangdong, 518055, P. R. China (phone: 86755-86392120; e-mail: wang.xx@siat.ac.cn).

Viorel Mihalef[2], is with Siemens Corporate Research, 755 College Road East, Princeton, N.J. 08540, U.S.A.

Zhen Qian, Szilard Voros[3] is with Piedmont Heart Institute, 95 Collier Rd, Suite 2085, Atlanta, GA, 30309, U.S.A.

Dimitris Metaxas[4], is with Computer Science Department, Rutgers University, 617 Bowser Road Piscataway, NJ, 08854, U.S.A.

model deformation. Section 3 presents the endocardial surface deformation results in a heart beating cycle. In section 4 we draw the conclusions and discuss possible improvements.

II. Procedure for Paper Submission

A. Segmentation

The 3D CT volume is first clustered with spatial and intensity information using the mean shift algorithm. Mean shift algorithm has the application such as edge preserving smoothing and image segmentation (Cosmaniciu 2002 [10,11]). Each pixel in the volume is projected to a space (x^s , x^r), where x^s is the spatial coordinates and with one more dimension x^r as the intensity. Each point in the 4D space is moving to the nearest densest place by updating the weighted average location in a kernel.

$$x_{new} = \frac{\sum_{i=1}^{n} x_i K(x_i)}{\sum_{i=1}^{n} K(x_i)} \tag{1}$$

where x_i is a point inside the kernel of x, K is the weight of point x_i in the kernel. The distance in space and the distance in intensity field are considered separately in the kernel weights

$$K_{h_s,h_r} = \frac{C}{h_s h_r} k\left(\left\|\frac{x^s}{h_s}\right\|^2\right) k\left(\left\|\frac{x^r}{h_r}\right\|^2\right) \tag{2}$$

where h_s and h_r are kernel bandwidths and C is the normalization constant. Clustered CT volume was thresholded into a binary volume. A 3D mesh consisting of triangular elements is generated along the surface with marching cubes algorithm.

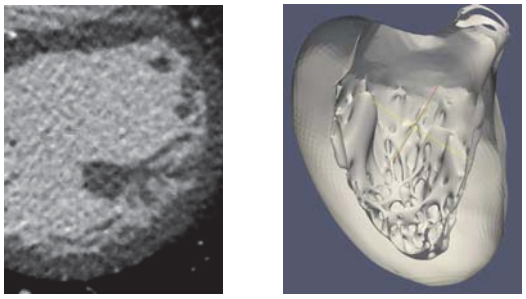

Figure 1. The original CT image on the left. The surface built with the mean shift clustering and marching cubes algorithm on the right.

B. Model Registration

The physical location of the heart can be obtained from the DICOM files. Anatomical landmarks such as aorta, ventricular septum cusps, high curvature points of right ventricle and other feature points are semi-automatically detected by curvature, equal space interval, and manual marking. 300 corresponding points are sampled on those landmarks. These point pairs provide long range external forces for meshless deformable models. The meshless deformable model fitting on the TMRI is shown in Figure 1.

Denote the generic model boundary landmarks as p_i, the TMRI contour landmarks as q_i. p_i^o and q_i^o are the model-centered coordinates, such as $p_i^o = p_i - \overline{p}_i, p_i \in V_1$. $T = \overline{p}_i - \overline{q}_i$ is the translation between the model and the image data. Assuming all the points are going on the same transformation, transformation matrix A can be calculated as in equation 7. When a generic heart mesh is registered onto the patient image data, assuming the transformation is the similarity transformation can avoid artifacts. The rotation can be isolated from the rest of the transformation with polar decomposition. The error function is the difference between image landmarks and transformed model landmarks. We minimize the error in equation 6 by setting its first derivative to zero, and yield equation 7.

$$E = \sum (Ap_i^o - q_i^o)^2 \tag{6}$$

$$A = (\sum_i p_i^o q_i^{o\prime})(\sum_i p_i^o p_i^{o\prime})^{-1} \tag{7}$$

Second term A_{pp} is a symmetric matrix, which only has the scaling information. The rotation matrix can be estimated by decomposing A_{pq}. A_{pq} can be decomposed to a rotation matrix R and a scaling matrix P. R is a unitary matrix and P is a positive-semidefinite Hermitian matrix. The singular value decomposition of A_{pq} can be written as $A_{pq} = W\Sigma V'$. W and V are unitary matrices describing rotation and Σ is a diagonal matrix describing the stretches in orthogonal axes. We have

$$P = V\Sigma V', \; R = WV' \tag{8}$$

If A is invertible, the rotation matrix of two sets of points can be calculated by substituting equation (10) into $R=A_{pq}P^{-1}$. After obtaining translation and rotation, uniform scaling can be deduced by comparing the average magnitude of vectors in the object-centered coordinates. The surface mesh generated from CT volume is registered onto the tagged MRI with the translation, rotation and uniform scaling.

$$P = \sqrt{A_{pq}^{'} A_{pq}} = \sqrt{(V\Sigma W')(W\Sigma V')} = \sqrt{V\Sigma V'} \tag{9}$$

$$P^{-1} = V(1/\Sigma)V' \tag{10}$$

C. Deformation with Deformable Models

In meshless deformable models, an object is represented as point clouds. Point locations are in heart coordinates and can be computed with parameterized functions. Tagging line tracking results [12] provide external forces for LV model deformation. Instead of grouping points with elements and keeping the shape with a stiffness matrix, points interact with each other through kernels.

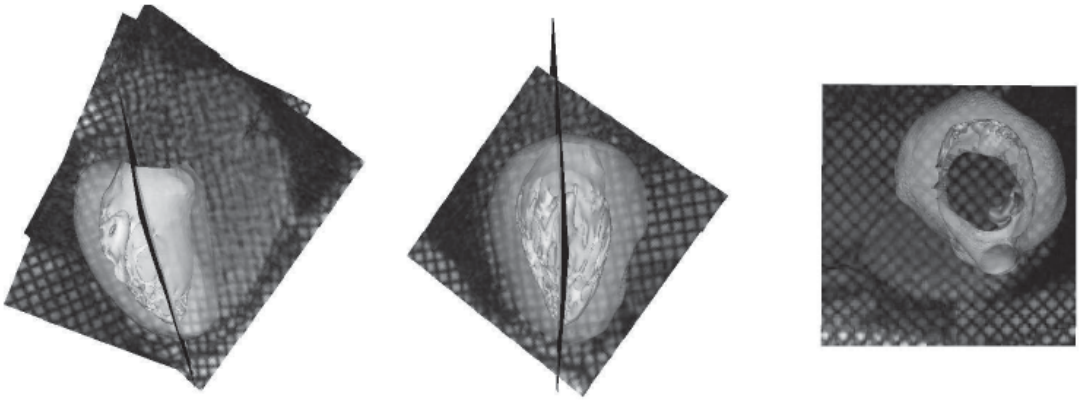

Figure 2. LV model with the endocardial surface reconstructed from CT data is registered

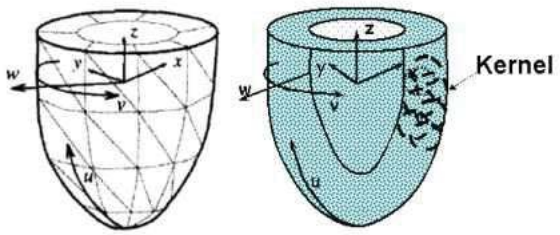

Figure 3. The left image is a mesh based deformable model. The right image is a meshless deformable model, in which the volume is represented by point clouds.

The left image is a mesh based deformable model. The right image is a meshless deformable model, in which the volume is represented by point clouds. They are both in prolate spheroidal coordinates and can be modeled by parameterized functions.

The Lagrangian equation for the model is

$$\dot{u} = f_{ext} + f_{int} \tag{11}$$

where u is the displacement of myocardium, u is the velocity, f_{ext} is the external force and f_{int} is the internal force. The internal force can be done with Laplacian coordinate local deformation. The velocity of a point in DICOM coordinates can be calculated as

$$\dot{u} = \mathrm{L}q \tag{12}$$

where **L** is the Jacobian matrix between point coordinates and parameters. With the Lagragian equation, the Jacobian matrix can be moved to the right side and the velocity of the variables q can be calculated. The external forces f_{ext} on parameters are integrated over the volume.

$$\dot{q} = f_q = \int_\Omega f_{ext}\mathrm{L} \tag{13}$$

The integration over the volume can be interpreted as the sum of the integrals over each kernel in the volume. The coordinates of particles in the meshless deformable model can be updated by recalculating parameterized function with the updated parameters, as in equation 12.

D. Local Laplacian Volume Deformation

After global deformation, the model is very close to its target shape. Laplacian Volume Deformation further refines the model locally, makes the material points converge to the locations in the next frame with small error threshold. We encode each point in the meshless deformable models into a Laplacian representation to keep the intrinsic geometric detail of myocardium. The Laplacian coordinates in a mesh describe the local geometric difference in Sorkine et al. [13]. We further extend it from a surface editing tool to a method for tracking geometric details of a volume.

The geometry of points on the model can be described as a set of differentials $\Delta = \{\delta_i\}$. The Laplacian coordinate of a point is the difference between the point location and the average of its neighbors' location.

$$\delta_i = v_i - \frac{1}{d_i}\sum_{|v_i - v_j|<h} v_j \tag{14}$$

The transformation can be described in a matrix form $\Delta = LV$, where $L = I - D^{-1}A$. A is the mesh adjacency matrix and $D = \{d_1, d_2, ..., d_n\}$ is the degree matrix. We combine landmarks and sampled points together to make a point set. Fixing the landmarks at the target locations v_{target} obtained from the next MRI frame, the rest of the free points deform to minimize the following error function.

$$E(V') = \sum_{i=1}^{n}\left\| T_i\,\delta_i - L(V_i')\right\|^2 + \sum_{j=1}^{m}\left\| v_j' - v_{target}\right\|^2 \tag{15}$$

where transformation T_i on each point is the unknown matrix and can be written as a linear function of V'. V' can be solved by minimizing the quadratic function. T_i is an approximation of the similarity transformation when the rotation angle is small. In our model, the major rotation is handled in the global deformation part. The small angle assumption of Laplacian deformation is made happen by iterations.

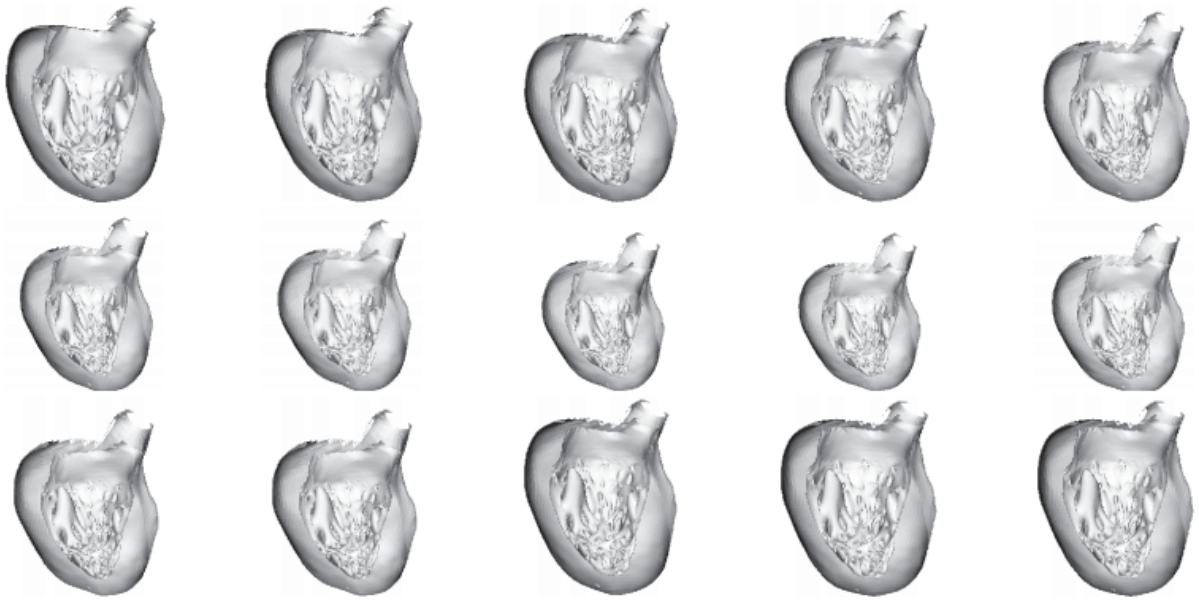

Figure 4. LV deformation results in the first half of a cardiac cycle.

III. Experimental Results

We applied our method to five different cardiac datasets. The CT images were acquired on a 320-MSCT scanner (Toshiba Aquilion ONE, Toshiba Medical Systems Corporation). This advanced diagnostic imaging system is the world's first dynamic volume CT scanner that captures a whole-heart scan in a single rotation, and achieves an isotropic 0.5mm volumetric resolution with much less motion artifact than the conventional 64-MSCT scanners. The created data had 512 by 512 by 330 pixels, with an effective atrio-ventricular region measuring about 300^3 pixels. In Figure 4, we show the 3D motion of LV surfaces generated from meshless deformable models. From the segmentation results, we can observe that most of trabeculae carneae are distributed on the free wall. Two papillary muscles of the LV are connected to the wall with roots. The reconstructed motion of the LV endocardial surfaces is more readily appreciated with such rendering than from the 3D volume. Two papillary muscles contract with the LV myocardium during the systole. At the end of systole, some of the trabeculae carneae clasp on the heart wall.

IV. Conclusion

We have developed a cardiac deformable model with all detailed anatomic structures on the LV endocardial surface with CT data, and have reconstructed the motion of the model with cues derived from tagged MRI. The reconstructed motion sequences show high agreement with cardiac video based on the comparison between the results and the live cardiac video.

References

[1] Leon Axel, "Papillary muscles do not attach directly to the solid heart wall," Circulation, vol. 109, pp. 3145–3148, 2004.

[2] T. Chen, D. N. Metaxas, and L. Axel, "3d cardiac anatomy reconstruction using high resolution CT data," in Int'l Conf. Medical Image Computing and Computer Assisted Intervention,, 2004, pp. 411–418.

[3] R. Ionasec, B. Georgescu, E. Gassner, S. Vogt, O. Kutter, M. Scheuering, N. Navab, and D. Comaniciu, "Dynamic model-driven quantitative and visual evaluation of the aortic valve from 4d CT," in Int'l Conf. Medical Image Computing and Computer Assisted Intervention,, 2008.

[4] Y. Zheng, A. Barbu, B. Georgescu, M. Scheuering, and D. Comaniciu, "Four-chamber heart modeling and automatic segmentation for 3d cardiac CT volumes using marginal space learning and steerable features," IEEE Trans. Medical Imaging, vol. 27, pp. 1668–1681, 2008.

[5] D. N. Metaxas and D. Terzopoulos, "Dynamic 3D models with local and global deformations: Deformable superquadrics.," IEEE Transaction on Pattern Analysis Machine Intelligence, vol. 13, no. 7, pp. 703–714, 1991.

[6] J. Park, D. Metaxas, and L. Axel, "Volumetric deformable models with parameter functions: A new approach to the 3D motion analysis of the LV from MRI-SPAMM," in ICCV, 1995, pp. 700–705.

[7] K. Park, D. N. Metaxas, and L. Axel, "A finite element model for functional analysis of 4D cardiac-tagged MR images," in Proceedings of MICCAI, 2003, pp. 491–498.

[8] X. Wang, T. Chen, D. Metaxas, and L. Axel, "Meshless deformable models for LV motion analysis," in CVPR, 2008.

[9] X. Wang, T. Chen, S. Zhang, D. Metaxas, and L. Axel, "LV motion and strain computation from TMRI based on meshless deformable models,", in MICCAI, 2008, vol. 1, pp. 636–644.

[10] D. Comaniciu, V. Ramesh, and P. Meer, "The variable bandwidth mean shift and data-driven scale selection," in IEEE Int. Conf. Computer Vision, 2001.

[11] D. Comaniciu and P. Meer, "Mean shift: A robust approach toward feature space analysis," IEEE Trans. Pattern Analysis Machine Intell., vol. 24, pp. 603–619, 2002.

[12] T. Chen, S. Chung, and L. Axel, "Automated tag tracking using gabor filter bank, robust point matching, and deformable models," Proceedings of Functional Imaging and Modeling of the Heart, pp. 22–31, 2007.

[13] O. Sorkine, Y. Lipman, D. Cohen-Or, M. Alexa, C. Rössl, and H. P. Seidel, "Laplacian surface editing," in Proceedings of the Eurographics/ACM SIGGRAPH, pp. 179–188